

Pile length estimation based on guided wave theory for unknown foundations

Shihao Cui, Hongwei Liu & Pooneh Maghoul
*Department of Civil, Geological and Mining Engineering– Polytechnique
Montréal, Montréal, Québec, Canada*



GeoCalgary
2022 October
2-5
Reflection on Resources

ABSTRACT

The construction of new structures on existing pile foundations can significantly reduce the overall project costs. The reuse of foundations requires information on the embedded depth of existing piles, which is not always known. In this paper, a new method based on the guided wave theory is proposed to effectively estimate the pile length of unknown foundations for the first time. In this method, a three-dimensional guided wave model of a cylindrical pile is built by the spectral element method. Then, a modified Ridders' algorithm is proposed to solve the spectrum relation obtained by the guide wave model. The phase difference of the two signals collected via two sensors placed on the lateral side of the test pile can be calculated. Based on the periodic analysis of the relationship between the phase difference and the wavenumber, the pile length can be determined. Finally, through the synthetic data, the effectiveness and accuracy of the proposed method are validated.

RÉSUMÉ

La construction de nouvelles structures sur des pieux existants peut réduire considérablement les coûts globaux du projet. La réutilisation des fondations nécessite des informations sur la profondeur d'encastrement des pieux existants, qui n'est pas toujours connue. Dans cet article, une nouvelle méthode basée sur la théorie des ondes guidées est proposée pour estimer efficacement la longueur des pieux de fondations inconnues pour la première fois. Dans cette méthode, un modèle d'onde guidée tridimensionnel d'un pieu cylindrique est construit par la méthode des éléments spectraux. Ensuite, un algorithme de Ridders modifié est proposé pour résoudre la relation spectrale obtenue par le modèle d'onde guide. La différence de phase des deux signaux collectés via deux capteurs placés sur le côté latéral du pieu d'essai peut être calculée. Sur la base de l'analyse périodique de la relation entre la différence de phase et le nombre d'onde, la longueur du pieu peut être déterminée. Enfin, à travers les données synthétiques, l'efficacité et la précision de la méthode proposée sont validées.

1 INTRODUCTION

There is a large number of unknown foundations and piles in urban and rural areas. As of 2005, around 60,000 bridges with an unknown foundation in the United States were identified (Yousefpour et al. 2014). It is most likely that more unknown foundations have not been identified or reported by the stakeholders (Stein and Sedmera 2006). In most cases, the as-built or design plans are no longer available. Hence, there is no information on the type, geometry, length, or bearing capacity of these foundations.

Reuse of foundations in new construction projects can significantly reduce the project costs and contribute to the sustainable development goals. Therefore, the characterization of unknown foundations and piles is of great importance. Pile length is an important indicator to determine the degree of scour and the bearing capacity of the pile (He et al. 2019).

Several methods have been proposed to evaluate unknown foundations and piles. These methods can mainly be divided into two categories: destructive testing and non-destructive testing (NDT). Destructive testing uses direct methods such as probing, auguring, drilling, or digging to possibly determine the properties of the foundation under investigation. Compared with destructive testing, NDT methods are preferred since they are cost-effective and safe. NDT methods can also be grouped into two types: surface methods and subsurface methods. In surface methods, both the load source and the response receivers

are placed at or near the ground surface from an accessible area of the foundation structure. The only requirement to perform the surface NDT tests is to have access to an exposed area of the foundation directly or on a member connected to the foundation (Gupta et al. 2021). In subsurface methods, at least one borehole (or called an access tube) is installed during construction alongside or within the bridge substructure. The incident signal is emitted into the test object (if needed) and is received by transducers placed within the borehole (Holla and Schabowicz 2010). The most popular subsurface methods include parallel seismic testing (PST), borehole radar testing (BRT), borehole sonic testing (BST), cross-hole sonic logging (CSL), thermal integrity profiling (TIP), etc. In comparison with subsurface methods, surface methods are highly praised because of the advantage of minimal intrusion, convenience, and lower cost.

For pile length estimation, in particular, numerous surface NDT techniques have been developed. For example, the Sonic echo (SE) and impulse response (IR) techniques are the earliest methods for pile length estimation. In these two methods, longitudinal stress (i.e. acoustic) waves are generated by an impact force on the top of the foundation. The stress waves will reflect at interfaces between materials with significant changes in acoustic impedance. As such, the responses collected by a nearby receiver(s) can be analyzed for the pile integrity analysis and pile length estimation. SE uses the responses in the time domain while IR utilizes the responses

transformed into the frequency domain (Jozi et al 2014). Based on the SE/IR techniques, some signal processing methods are applied to improve the accuracy for pile length estimation. Kim et al (2020) used the conventional non-linear amplification method and wavelet packet transform to process the impact echo data for pile defect detection. Ni et al. (2012) utilized the continuous wavelet transform to enhance the characteristics of the echo signals and the proposed method is used for pile or drilled shaft length estimation and pile integrity test. Ultra-seismic testing (UST) has been also used to determine the length of piles. In this technique, multiple receivers are mounted on the side of the exposed part of the test pile and the same way of excitation used in SE or IR can be utilized here. Wang and Hu (2015) utilized the UST method with electrical resistivity tomography to estimate the depth of the concrete foundation on two bridges.

The bending wave-based method is proposed to address the case when the top pile is not accessible. In this technique, the lateral impact is applied to the exposed part of the test pile, and the dispersive or bending waves can be generated. The short kernel method (SKM) was proposed by Douglas and Holt (1993) for data collection. This method does not perform well for piles buried in deep embeddings. Some signal processing methods are then used to process the responses collected on the lateral side for pile length estimation, such as Hilbert Huang transform (Farid 2012) and complex continuous wavelet transform (Ni et al 2019). Samu and Guddati (2019 and 2020) proposed a spectral method that maps the wavenumber and the phase difference. This method provides a simple way for pile estimation by observing the plot of the wavenumber and the phase difference. However, since the dispersion relation theory used here is based on a one-dimensional (1D) beam model, the accuracy is limited, and especially when the embedded depth of the pile is deep, the accuracy is worse.

In this paper, a new pile length estimation method is proposed by combing the phase difference analysis and the 3D guided wave theory for the first time. The guided wave-based dispersion relation is obtained by the spectral element method (SEM). A modified Ridders' algorithm is proposed for the root-searching of the spectrum relation determined by the guided wave model. The spectrum relation is then used to form the dispersion analysis diagram of the wavenumber with regard to the phase difference. According to the relation between the wavenumber and phase difference calculated by collected lateral vibration responses, the pile length can be estimated. Through numerical analysis, the effectiveness and the accuracy of the proposed method can be validated. More particularly, the proposed method shows a good accuracy in estimating the length of deep foundations.

2 METHODOLOGY

2.1 Methodology overview

The holistic process of the proposed method for pile length estimation based on the phase difference analysis and the 3D guided wave model is shown in Figure 1.

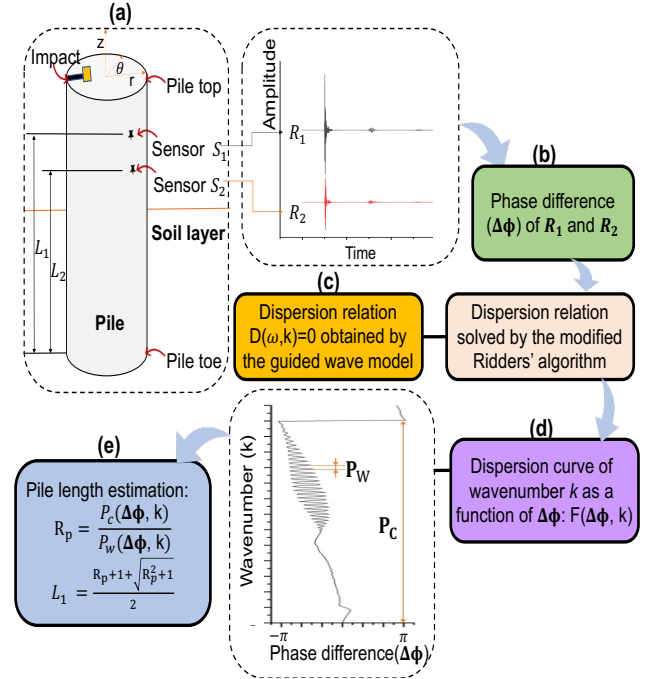


Figure 1. The schematic flowchart of the proposed methodology.

2.2 Experimental setup and data acquisition

The schematic diagram of the experiment setup for pile length estimation using the lateral-side responses and the top-surface responses is shown in Figure 1(a). For a pile under investigation, if there is an exposed part, the signals at the lateral-side can be used. In this case, two sensors, denoted by S_1 and S_2 , are placed on the lateral side of the exposed part of the pile. The distance between S_1 and the pile toe, and the distance between S_2 and the pile toe, are denoted by L_1 and L_2 , respectively. In this case, the impact can be applied on the pile top. The vibration responses acquired by the sensors S_1 and S_2 are denoted by R_1 and R_2 , respectively.

2.3 Phase difference calculation

The signal R_1 and R_2 in the time domain can be transferred into the frequency domain by the Fast Fourier transform, and the corresponding signals in the frequency domain are denoted by $R_1(\omega)$ and $R_2(\omega)$, respectively. The phase difference of these two signals, denoted by $\Delta\phi$, can be defined as,

$$\Delta\phi = \text{Imag}(\log(R_1(\omega)) - \log(R_2(\omega))), \quad [1]$$

where $\text{Imag}(\cdot)$ means the imaginary part of the input signal and $\log(\cdot)$ is the logarithmic function; the phase difference can be transferred into the range $[-\pi, \pi]$.

2.4 Spectrum relation of a cylindrical pile

The propagation of the guided wave follows the Navier-Stokes equation,

$$(\lambda + \mu)\nabla\nabla \cdot \mathbf{u} + \mu\nabla^2\mathbf{u} = \rho \frac{\partial^2\mathbf{u}}{\partial t^2}. \quad [2]$$

In this equation, \mathbf{u} is the displacement field; ρ is the density of the material of the pile; λ and μ are the Lamé coefficients, which can be calculated as

$$\lambda = \frac{Ev}{(1+\nu)(1-2\nu)}, \mu = \frac{E}{2(1+\nu)} \quad [3]$$

in which E is the Young's modulus; ν is the Poisson's ratio of the pile material. The Helmholtz's decomposition can be used to solve the displacement field \mathbf{u} , which can be represented by two potentials ϕ and $\boldsymbol{\psi}$. ϕ is the scalar longitudinal component and $\boldsymbol{\psi}$ is the shear vector component. There is,

$$\mathbf{u} = \nabla\phi + \nabla \times \boldsymbol{\psi} \quad [4]$$

where $\nabla \cdot \boldsymbol{\psi} = \mathbf{0}$. Based on the Bessel function, the displacement \mathbf{u} can be estimated by

$$u_r = [k_s J_1(k_s r)A + ik J_1(k_p r)B]e^{i(kz - \omega t)}, \quad [5a]$$

$$u_z = [ik J_0(k_s r)A + k_p J_0(k_p r)B]e^{i(kz - \omega t)}, \quad [5b]$$

in which k is the wavenumber and ω is the angular frequency. u_r and u_z are the displacement in r and z directions, respectively; r and z are the variables in the cylindrical coordinate system; $J_0(\cdot)$ and $J_1(\cdot)$ are the first kind Bessel functions at the order 0 and 1, respectively. The relation between the stress components and the displacement components are as follows,

$$\sigma_{rz} = \mu \left(\frac{\partial u_r}{\partial z} + \frac{u_z}{r} \right), \quad [6a]$$

$$\sigma_{zz} = \left(\frac{\partial u_r}{\partial r} + \frac{u_z}{r} + \frac{\partial u_z}{\partial z} \right) + 2\mu \frac{\partial u_z}{\partial z}. \quad [6b]$$

Substituting Equation 5 into Equation 6, the stress in different directions can be calculated. According to the free traction condition of the cylindrical pile, i.e., $\sigma_{rz} = \sigma_{zz} = 0$, the following equation can be obtained,

$$\mathbf{M}[A, B]^T = \mathbf{0}. \quad [7]$$

where $\mathbf{M} = \begin{bmatrix} m_{11} & m_{12} \\ m_{21} & m_{22} \end{bmatrix}$; $m_{11} = -(\lambda k^2 + \lambda k_s^2 + 2\mu k_s^2)J_0(k_s r) + 2\mu k_s J_1(k_s r)/r$; $m_{12} = -2\mu i k k_p J_0(k_p r) + 2\mu i J_1(k_p r)/r$; $m_{21} = -2\mu i k k_s J_1(k_s r)$; $m_{22} = \mu(k^2 - k_p^2)J_1(k_s r)$; r is the radius of the pile; k_s and k_p are the wavenumber of the shear and the longitudinal wave respectively. There is,

$$k_s^2 = \frac{\omega}{c_s^2} - k^2, \quad [8a]$$

$$k_p^2 = \frac{\omega}{c_p^2} - k^2, \quad [8b]$$

Here c_s and c_p are the shear and longitudinal wave velocity, respectively. Let the homogenous linear equation have the non-zero solution, the determinant of \mathbf{M} should be equal to 0, i.e., $|\mathbf{M}| = 0$. Therefore, the spectrum relation

between the wavenumber k and the angular frequency ω can be built, denoted by $D(\omega, k) = 0$. Accordingly, this equation can be solved by a root-searching algorithm. In this paper, a modified Ridders' algorithm is proposed for this purpose.

2.5 Modified Ridders' algorithm

When the spectrum relation is built, the modified Ridders' algorithm shown in Figure 2 is used for root-searching. In this algorithm, Ω is the given frequency vector, and V_{ph} is the phase velocity, and it can be initialized by the dispersion relation curve distribution; $step_length$ is the step length of iteration for phase velocity (here it is set as 0.2). N_{step} is the pre-defined maximum iteration number and it is set as 10^6 .

The design of this algorithm is that at first a range formed by two variables with opposite signs is searched by iteration; then Ridders' algorithm is used to perform precise searching in the range. K_Ω is the vector recording the wavenumber found by the proposed method at each frequency in the frequency vector Ω .

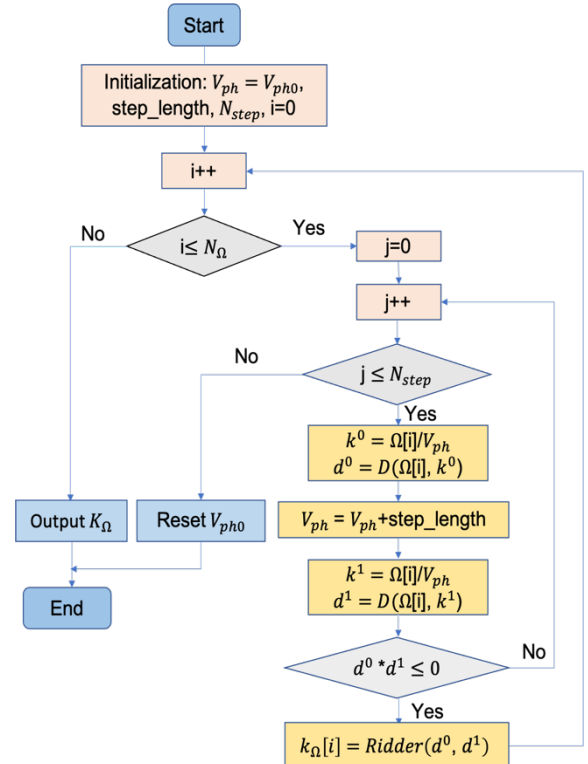


Figure 2. The flowchart of the modified Ridders' root-searching algorithm.

2.6 Pile length estimation based on the dispersion analysis

Equation 5 gives the general solution of displacement of the guided wave, and here the component u_z is used as an example to show the analysis process for pile length estimation. According to Equation 5b, and the definition of

phase difference (Equation 1), the phase difference of two signals collected at the position L_1 and L_2 can be calculated as,

$$\Delta\phi = k\Delta z, \quad [9]$$

where $\Delta z = L_1 - L_2$, and the reflected wave is not taken into consideration. When the reflected wave is considered, the displacement u_z can be written as,

$$u_z = [ikJ_0(k_s r)A_1 + k_p J_0(k_p r)B_1]e^{i(kz)} + [ikJ_0(k_s r)A_2 + k_p J_0(k_p r)B_2]e^{i(-kz)}, \quad [10]$$

where A_1 and B_1 are the unknown coefficients responsible for the incident wave and A_2 and B_2 are the unknown coefficients responsible for the reflected wave. According to the definition of the phase difference, and the Euler's formula, the two signals collected at the position L_1 and L_2 can be simplified as,

$$\Delta\phi = k\Delta z + \tan^{-1}(\phi(L_2)) - \tan^{-1}(\phi(L_1)) \quad [11]$$

where $\tan^{-1}(\cdot)$ is the inverse tangent function, and

$$\phi(z) = \frac{A_2 + A_1 \cos 2kz}{Q_{temp}(B_2 + B_1 \cos 2kz) - A_1 \sin 2kz} + \frac{B_1 \sin 2kz}{(B_2 + B_1 \cos 2kz) - A_1 \sin 2kz / Q_{temp}} \quad [12]$$

where $\phi(z)$ is a phase-related function and the value of Q_{temp} is close to the constant 1. Because of this, it can be regarded as a periodic trigonometric function and its period can be estimated as $\frac{\pi}{z}$. Therefore, the second and third terms in Equation [11] can also be regarded as periodic functions, and their periods are $\frac{\pi}{L_2}$ and $\frac{\pi}{L_1}$, respectively. Therefore, we can estimate the pile length by the position of the sensors placed at L_1 and L_2 according to the periodic analysis obtained from the phase difference.

The periodic analysis is as follows. Two signals are considered: signal with reflections, which corresponds to Equation 9, in which we can observe its saw-tooth waveform and the period P_c is defined as shown in Figure 3. The angle θ in the figure is the slope of the curve. As it can be seen in Equation 9, the slope of the curve can also be related to Δz . Therefore,

$$\tan\theta = \frac{\pi}{P_c(\Delta\phi, k)} = \Delta z \quad [13]$$

As such, one obtains

$$P_c(\Delta\phi, k) = \frac{\pi}{\Delta z} \quad [14]$$

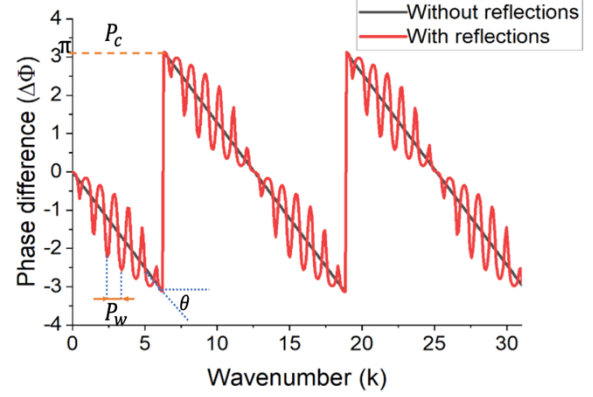


Figure 3. The dispersion analysis diagram of the example signal to observe the period.

From Figure 3, it can also be seen that the signal with reflections brings small oscillations or wiggles on the curve without reflections. The period of wiggles is defined as $P_w(\Delta\phi, k)$. According to the analysis in Equation 12, the period of the wiggle can be estimated as the average of $\frac{\pi}{L_2}$ and $\frac{\pi}{L_1}$, i.e.,

$$P_w(\Delta\phi, k) = \left(\frac{\pi}{L_2} + \frac{\pi}{L_1}\right)/2 \quad [15]$$

Then the quotient of the period can be calculated as,

$$R_p = \frac{P_c(\Delta\phi, k)}{P_w(\Delta\phi, k)} \quad [16]$$

According to the relation of L_1 , L_2 and Δz , L_1 can be estimated as,

$$L_1 = \left(\frac{R_p + 1 + \sqrt{R_p^2 + 1}}{2}\right) \Delta z \quad [17]$$

From Equation 17, because Δz is known, and R_p can be obtained by the two period which can be identified in the dispersion analysis diagram, the pile length can be estimated by the sensor position L_1 .

3 VALIDATION

In this work, the synthetic data is generated by a commercial finite element software. Three piles buried in the soil are studied here. The physical properties and the radius of the test pile are presented in Table 1. The pile length and the position of the sensors placed on the lateral side for each pile are given in Table 2.

Table 1. The physical property and the radius of the test pile

Parameter (unit)	Value
Density $\rho(\text{kg}/\text{m}^3)$	2200
Poisson's ratio	0.25
Young's modulus (GPa)	18.77
Radius (m)	0.5

Table 2. The pile length and the sensor position for each case

Parameter (unit)	Pile 1	Pile 2	Pile 3
Pile length $L(\text{m})$	15	20	30
Sensor position, $L_1(\text{m})$	14.5	19.5	29.5
Sensor position, $L_2(\text{m})$	14.2	19.2	29.2
Sensor distance, $\Delta z(\text{m})$	0.3	0.3	0.3

In the simulation, the Ricker wavelet is used as the excitation function, and the excitation frequency is set as 10 kHz. The sampling rate is 10^5 Hz , and the sampling rate 0.05 s, so for each sensor a time-series signal with 5,000 samples can be obtained. The vibration signal collected here is the velocity. The spectrum relation is obtained by $D(\omega, k) = 0$ built in Equation 7.

Figure 4 shows the first five branches of the dispersion relation. The dispersion relation is the relation between the phase velocity (v) and the angular frequency (ω), which can be converted by the spectrum relation, using $v = \frac{\omega}{k}$. In this figure, q indicates the branch number; p indicates the mode type of the guided wave, p=0 indicates the dispersion relation using the longitudinal mode, and L refers to the longitudinal mode. When the impact is placed on the pile top, the longitude mode of the guided wave should be used and the first branch dispersion L (0,1) is the predominant one among all branches (Chao 2002). In the low-frequency range, only the dispersion relation L (0,1) exists. Therefore, the branch L (0,1) is selected for pile length estimation.

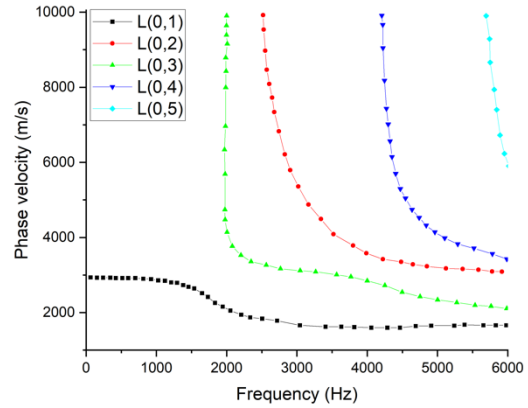


Figure 4. The first 5 branches of the dispersion relation of the test pile.

The dispersion analysis diagram can be obtained using the phase difference of the two signals collected on the lateral side of each pile. According to the spectrum relation L (0,1) in Figure 4, the dispersion analysis diagram to show the relation between the wavenumber k and the phase difference can be obtained. The dispersion relation diagram for each pile has been shown in Figure 5. From the curve of each pile, it can be observed that the cycle period can be clearly obtained, and a series of wiggles can also be identified. According to this figure, in each curve, the cycle period $P_c(\Delta\phi, k)$ and the wiggle period $P_w(\Delta\phi, k)$ can be identified. The wiggle period $P_w(\Delta\phi, k)$ can be read at the different wavenumber, to get a stable value, the average of those values with the outlier removed can be used to indicate the wiggle period $P_w(\Delta\phi, k)$. Then according to Equation 17, the position of the sensor position L_1 can be estimated.

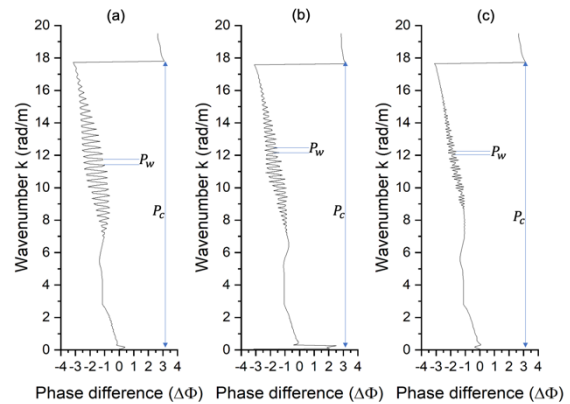


Figure 5. The dispersion analysis diagram of the three piles. (a). Pile 1. (b). Pile 2. (c). Pile 3.

Since the distance between the sensor S_1 and the pile top is known in the exposed part of the test pile, therefore

the pile length can be determined by the estimated value L_1 . The error rate of the estimation result for each pile is given in Table 3. The result shows the proposed method can achieve an accurate estimation of the pile length. Therefore, the effectiveness and accuracy of the proposed method can be validated.

Table 3. The result of the absolute error rate

Piles	Absolute error rate
Pile 1	0.023
Pile 2	0.035
Pile 3	0.039

4 CONCLUSION

This paper proposes a novel pile length estimation method based on the guided wave theory and the phase difference analysis of two signals collected on the lateral side of the test pile. The guided wave theory-based dispersion relation is built by the spectral element method, and the modified Ridders' algorithm is proposed to perform the root-searching of the dispersion relation. According to the analysis of the phase difference, the periodic pattern of the dispersion analysis diagram of the wavenumber as a function of the phase difference is then used for pile length estimation. Future work should be focused on the case where the signals can only be collected on the top surface, or how to estimate the pile length when only one signal is used for pile length estimation.

5 REFERENCES

Douglas, R.A. and Holt, J.D. 1993. Determining length of installed timber pilings by dispersive wave propagation methods. Report for the Center for Transportation Engineering Studies, North Carolina State University.

Farid, A.T.M. 2012. Prediction of unknown deep foundation lengths using the hilbert huang transform (hht). *HBRC Journal*, 8(2):123–131.

Gupta, M., Khan, M.A., Butola, R., and Singari, R. 2021. Advances in applications of non-destructive testing (ndt): A review. *Advances in Materials and Processing Technologies*, 1:1–22.

He, B., Lai, Y., Wang, L., Hong, Y., and Zhu, R. 2019. Scour effects on the lateral behavior of a large-diameter monopile in soft clay: Role of stress history. *Journal of Marine Science and Engineering*, 7(6):170.

Hola, J. and Schabowicz, K. 2010. State-of-the-art non-destructive methods for diagnostic testing of building structures – anticipated development trends. *Archives of Civil and Mechanical Engineering*, 10(3):5–18.

Jozi, B.J., Dackermann, U., Braun, R.B., Li, J., and Samali, B.S. 2014. Application and improvement of conventional stress-wave-based non-destructive testing methods for the condition assessment of in-service timber utility poles. In *Australasian Conference on the Mechanics of Structures and Materials*. Southern Cross University, 1:1197-1202.

Kim, H., Mission, J., Dinoy, P.R., Kim, H. and Park, T. 2020. Guidelines for impact echo test signal interpretation based on wavelet packet transform for the detection of pile defects. *Applied Sciences*, 10(7): 1-23.

Ni, S., Isenhowe, W.M., and Huang, Y. 2012. Continuous wavelet transform technique for low-strain integrity testing of deep drilled shafts. *Journal of GeoEngineering*, 7(3):97–105.

Ni, T., Tsai, P., Yang, Y. and Chou, W. 2019. Improved approach for determining pile length of group pile using complex continuous wavelet transform. *Journal of Testing and Evaluation*, 47:20170720.

Samu, V. and Guddati, M. 2019. Nondestructive method for length estimation of pile foundations through effective dispersion analysis of reflections. *Journal of Nondestructive Evaluation*, 38(2):1–11.

Samu, V. and Guddati, M. 2020. Nondestructive length estimation of an embedded pile through combined analysis of transverse and longitudinal waves. *NDT & E International*, 110:102203.

Stein, S. and Sedmera, K. 2006. Guidelines for risk-based management of bridges with unknown foundations. In *World Environmental and Water Resources Congress 2006*, Springfield, VA, USA, 1:1–10.

Wang, H. and Hu, C. 2015. Identification on unknown bridge foundations using geophysical inspecting methods. *The e-Journal of Nondestructive Testing*, 20(11):905–912.

Yousefpour, N., Medina-Cetina, Z, and Briaud, J.L. 2014. Evaluation of unknown foundations of bridges subjected to scour: Physically driven artificial neural network approach. *Transportation Research Record*, 2433(1):27–38.